

# Imaginary potential and thermal width in the spinning black hole background from holography

Zhou-Run Zhu,<sup>1,\*</sup> Sheng Wang,<sup>2,†</sup> Yang-Kang Liu,<sup>2,‡</sup> and Defu Hou<sup>2,§</sup>

<sup>1</sup>*School of Physics and Telecommunications Engineering,  
Zhoukou Normal University, Zhoukou 466001, China*

<sup>2</sup>*Institute of Particle Physics and Key Laboratory of Quark and Lepton Physics (MOS),  
Central China Normal University, Wuhan 430079, China*

## Abstract

In this study, we investigate the imaginary potential and thermal width of heavy quarkonium in the spinning black hole background. Using a holographic approach, we systematically analyze how angular momentum influences these quantities. Our results reveal that increasing angular momentum causes the imaginary potential to emerge at smaller interquark distances, suggesting that angular momentum accelerates quarkonium melting. Furthermore, we find that angular momentum enhances the thermal width, indicating greater instability of the bound state at higher angular momentum. Notably, we observe that the effect of angular momentum on quarkonium dissociation is more pronounced when the axis of the quark-antiquark pair is transverse to the direction of angular momentum.

---

\* [zhuzhourun@zknu.edu.cn](mailto:zhuzhourun@zknu.edu.cn)

† [shengwang@mails.ccnu.edu.cn](mailto:shengwang@mails.ccnu.edu.cn)

‡ [ykl@mails.ccnu.edu.cn](mailto:ykl@mails.ccnu.edu.cn)

§ [houdf@mail.ccnu.edu.cn](mailto:houdf@mail.ccnu.edu.cn)

## I. INTRODUCTION

Heavy quarkonium consists of a heavy quark and a heavy antiquark, serving as a powerful probe for understanding the properties of quark-gluon plasma (QGP). The melting of heavy quarkonium is one of the primary experimental indications of the formation of QGP. One direct evidence of this is the suppression of heavy quarkonium due to the color screening [1]. Another reason for the suppression is the imaginary part of the potential. Some related researches [2–4] have suggested that the imaginary potential may play a more critical role in explaining thermal properties of quarkonium within the strongly coupled medium. The imaginary potential can explain the dissociation and decay of the bound state. Additionally, it can be used to estimate the thermal width of quarkonium related to thermal decay [5–7].

The non-central heavy ion collisions experiments have shown the generation of nonzero angular momentum [8–12]. While part of the angular momentum is carried away by spectator partons, a significant portion is transferred to the strongly coupled plasma [13, 14]. In [11], the results from Star Collaboration on the  $\Lambda$  and  $\Lambda^-$  baryons provide strong evidence and yield an angular velocity average value  $\omega \sim 6$  MeV. The prediction of heavy-ion collisions hydrodynamic simulations [12] suggests that the magnitudes of angular velocity can be larger,  $\omega \sim (20\text{-}40)$  MeV. These nonzero angular velocity values result in relativistic rotation of the strongly coupled plasma. Investigating the influence of rotation on the thermodynamics of heavy quarkonium is an attractive research topic.

AdS/CFT correspondence [15–17] serves as a powerful non-perturbative method for investigating the properties of strongly coupled systems and offers valuable insights into the behavior of heavy quarks in strongly coupled plasma. In the context of holography, quarks correspond to the endpoints of open strings that are embedded in the bulk of anti-de Sitter (AdS) spacetime. A quark-antiquark pair is represented by a string that connects the two endpoints. This string forms on a U-shaped configuration, and its dynamics are described by the Nambu-Goto action. By using AdS/CFT correspondence, Noronha and Dumitru first calculate the imaginary potential in  $\mathcal{N} = 4$  super-Yang Mills (SYM) theory from thermal fluctuation [18]. The study of the imaginary potential of heavy quarkonium has gained significant attention. The imaginary potential and thermal width in the static background has been discussed in [19]. Additionally, the imaginary potential in the moving cases has been studied in [20, 21]. In Ref. [22, 23], the authors investigate the influence of finite 't Hooft

coupling corrections on the imaginary potential and the thermal width. The imaginary potential and the thermal width within AdS/QCD can be seen in [24–26]. The imaginary potential in the rotating matter has been studied in [27]. In Ref. [28], the authors explore the imaginary potential in the anisotropic plasma. Other related works can be seen in [29–34].

In this work, we want to explore the impact of angular momentum on the imaginary potential and thermal width from holography. It should be mentioned that the authors of Ref. [27] extend the static black hole to a local rotating by the Lorentz transformation [35–37], and calculate the imaginary potential in the rotating background. From this Lorentz transformation, the resulting black hole is a (hyper) cylindrical surface about the symmetry axis, and just represents a small area around the rotating radius  $L$  with a domain range less than  $2\pi$ . It is meaningful to examine the imaginary potential and thermal width within the spinning black hole background [38–42]. As discussed in [41], Myers-Perry black holes (spinning black hole) are the solutions in higher-dimensional spacetimes under Einstein gravity, which describe a rotating black hole with independent angular momentum. The boundary of the spacetime is typically compact, which leads to a gauge theory that lives on a spacetime  $S^3 \times \mathbb{R}$ . When considering large black holes in high-temperature regimes, the spacetime geometry tends to a planar geometry  $\mathbb{R}^{3,1}$ . The black hole can be described by a planar black brane solution, where the asymptotic boundary is no longer compact but instead non-compact and flat. In the dual field theory, the planar black brane is particularly relevant for understanding the behavior of the QGP. Inspired by this, we aim to examine the impact of angular momentum on the imaginary potential and thermal width in the Myers-Perry black hole background.

The paper is organized as follows. In Sec. II, we briefly review the spinning black hole background. In Sec. III, we explore the imaginary potential and thermal width of heavy quarkonium in spinning black hole background. In Sec. IV, we give the conclusion and discussion.

## II. SPINNING MYERS-PERRY BLACK HOLE BACKGROUND

In this work, we aim to investigate the influence of angular momentum on the imaginary potential and thermal width of heavy quarkonium. We first briefly review the metric of five-dimensional spinning black hole background, which is proposed by Hawking et al [38]

$$\begin{aligned}
ds^2 = & -\frac{\Delta}{\rho^2}(dt_H - \frac{a \sin^2 \theta_H}{\Xi_a} d\phi_H - \frac{b \cos^2 \theta_H}{\Xi_b} d\psi_H)^2 \\
& + \frac{\Delta_{\theta_H} \sin^2 \theta_H}{\rho^2} (adt_H - \frac{r_H^2 + a^2}{\Xi_a} d\phi_H)^2 + \frac{\Delta_{\theta_H} \cos^2 \theta_H}{\rho^2} (bdt_H - \frac{r_H^2 + b^2}{\Xi_b} d\psi_H)^2 + \frac{\rho^2}{\Delta} dr_H^2 \\
& - \frac{\rho^2}{\Delta_{\theta_H}} d\theta_H^2 + \frac{1 + \frac{r_H^2}{L^2}}{r_H^2 \rho^2} (abd t_H - \frac{b(r^2 + a^2) \sin^2 \theta_H}{\Xi_a} d\phi_H - \frac{a(r^2 + b^2) \cos^2 \theta_H}{\Xi_b} d\psi_H)^2,
\end{aligned} \tag{1}$$

with

$$\begin{aligned}
\Delta &= \frac{1}{r_H^2} (r_H^2 + a^2)(r_H^2 + b^2)(1 + \frac{r_H^2}{L^2}) - 2M, \\
\Delta_{\theta_H} &= 1 - \frac{a^2}{L^2} \cos^2 \theta_H - \frac{b^2}{L^2} \sin^2 \theta_H, \\
\rho &= r_H^2 + a^2 \cos^2 \theta_H + b^2 \sin^2 \theta_H, \\
\Xi_a &= 1 - \frac{a^2}{L^2}, \\
\Xi_b &= 1 - \frac{b^2}{L^2},
\end{aligned} \tag{2}$$

where  $a$  and  $b$  are the angular momentum parameters. In this work, we consider spinning Myers-Perry black hole case, namely  $a = b$  case [39, 40]. In addition,  $\phi_H$ ,  $\psi_H$  and  $\theta_H$  represent angular Hopf coordinates.  $t_H$  denotes time,  $L$  is the AdS radius, and  $r_H$  represents AdS radial coordinate.  $M$  is the mass.

After adopting the more convenient coordinates [43]

$$\begin{aligned}
t &= t_H, \\
r^2 &= \frac{a^2 + r_H^2}{1 - \frac{a^2}{L^2}}, \\
\theta &= 2\theta_H, \\
\phi &= \phi_H - \psi_H, \\
\psi &= -\frac{2at_H}{L^2} + \phi_H + \psi_H, \\
b &= a, \\
\mu &= \frac{M}{(L^2 - a^2)^3},
\end{aligned} \tag{3}$$

one can rewrite the metric (1) as

$$ds^2 = -(1 + \frac{r^2}{L^2}) dt^2 + \frac{dt^2}{G(r)} + \frac{r^2}{4} ((\sigma^1)^2 + (\sigma^2)^2 + (\sigma^3)^2) + \frac{2\mu}{r^2} (dt + \frac{a}{2} \sigma^3)^2, \tag{4}$$

with

$$\begin{aligned}
G(r) &= 1 + \frac{r^2}{L^2} - \frac{2\mu(1 - \frac{a^2}{L^2})}{r^2} + \frac{2\mu a^2}{r^4}, \\
\mu &= \frac{r_h^4(L^2 + r_h^2)}{2L^2 r_h^2 - 2a^2(L^2 + r_h^2)}, \\
\sigma^1 &= -\sin\psi dt d\theta + \cos\psi \sin\theta d\phi, \\
\sigma^2 &= \cos\psi d\theta + \sin\psi \sin\theta d\phi, \\
\sigma^3 &= d\psi + \cos\theta d\phi,
\end{aligned} \tag{5}$$

where

$$-\infty < t < \infty, \quad r_h < r < \infty, \quad 0 \leq \theta \leq \pi, \quad 0 \leq \phi \leq 2\pi, \quad 0 \leq \psi \leq 4\pi. \tag{6}$$

The planar black brane can be obtained by the coordinate transformation [41]

$$\begin{aligned}
t &= \tau, \\
\frac{L}{2}(\phi - \pi) &= x_1, \\
\frac{L}{2}\tan(\theta - \frac{\pi}{2}) &= x_2, \\
\frac{L}{2}(\psi - 2\pi) &= x_3, \\
r &= \tilde{r},
\end{aligned} \tag{7}$$

where  $(\tau, \tilde{r}, x_1, x_2, x_3)$  denote new coordinates. These coordinates can be scaled with a factor  $\beta$

$$\begin{aligned}
\tau &\rightarrow \beta^{-1}\tau, \\
x_1 &\rightarrow \beta^{-1}x_1, \\
x_2 &\rightarrow \beta^{-1}x_2, \\
x_3 &\rightarrow \beta^{-1}x_3, \\
\tilde{r} &\rightarrow \beta\tilde{r}, \\
\tilde{r}_h &\rightarrow \beta\tilde{r}_h. (\beta \rightarrow \infty)
\end{aligned} \tag{8}$$

One can derive the metric of a Schwarzschild black brane, which is boosted in the  $\tau - x_3$  plane [41]

$$ds^2 = \frac{r^2}{L^2}(-d\tau^2 + dx_1^2 + dx_2^2 + dx_3^2 + \frac{r_h^4}{r^4(1 - \frac{a^2}{L^2})}(d\tau + \frac{a}{L}dx_3)^2) + \frac{L^2 r^2}{r^4 - r_h^4} dr^2, \tag{9}$$

where the Schwarzschild black brane can be recovered when angular momentum vanishes ( $a = 0$ ).

Then, we take  $z$  ( $r = 1/z$ ) as the holographic fifth coordinate for simplified calculations

$$ds^2 = \frac{1}{z^2 L^2} [-d\tau^2 + dx_1^2 + dx_2^2 + dx_3^2 + \frac{z^4}{z_h^4(1 - \frac{a^2}{L^2})}(d\tau + \frac{a}{L}dx_3)^2] + \frac{L^2 z_h^4}{z^2(z_h^4 - z^4)} dz^2. \quad (10)$$

The expression of temperature is [41]

$$T_h = \frac{\sqrt{L^2 - a^2}}{z_h \pi L^3}, \quad (11)$$

where  $z_h$  denote the horizon. In the following calculations, we take AdS radius  $L = 1$  for simplicity. In the limitation of the large black hole, the angular velocity  $\Omega = a/L^2$  [41].

### III. IMAGINARY POTENTIAL AND THERMAL WIDTH IN SPINNING MYERS-PERRY BLACK HOLE BACKGROUND

In this section, we explore the imaginary potential and thermal width of heavy quarkonium in the spinning background, which could be calculated from the on-shell action of world sheet. The formulas for imaginary potential and thermal width can be derived by following the steps in Ref. [18, 19, 28].

The on-shell Nambu-Goto action is

$$S = -\frac{1}{2\pi\alpha'} \int d\tau d\sigma \sqrt{-\det g_{\alpha\beta}}, \quad (12)$$

where  $g_{\alpha\beta}$  is the determinant of induced metric.  $\tau$  and  $\sigma$  represents the world sheet coordinates.

In the following discussion, we will explore the impact of angular momentum in different directions. The gravitational metric can be viewed as boosted in the  $\tau - x_3$  plane, indicating that the direction of rotation is along the  $x_3$  direction. Meanwhile, the axis of the  $Q\bar{Q}$  pair in the  $x_1 - x_2$  plane is considered a transverse case, whereas the axis of the  $Q\bar{Q}$  pair aligned with the  $x_3$  is regarded as a parallel case.

In transverse case, the world sheet coordinates can be parameterized by

$$\tau = \xi, \quad x_1 = \eta, \quad x_2 = 0, \quad x_3 = 0, \quad z = z(\eta), \quad (13)$$

The Lagrangian density can be obtained as

$$\mathcal{L} = \sqrt{A(z) + B(z)\dot{z}^2}, \quad (14)$$

with

$$A(z) = A(z_\perp) = \frac{1}{z^4} - \frac{1}{z_h^4(1-a^2)}, \quad B(z) = B(z_\perp) = \frac{z_h^4}{z^4(z_h^4-z^4)} - \frac{1}{(z_h^4-z^4)(1-a^2)}. \quad (15)$$

In parallel case, the world sheet coordinates can be parameterized by

$$\tau = \xi, \quad x_1 = 0, \quad x_2 = 0, \quad x_3 = \eta, \quad z = z(\eta). \quad (16)$$

The expressions of  $A(z)$  and  $B(z)$  are

$$A(z) = A(z_\parallel) = \frac{z_h^4 - z^4}{z^4 z_h^4}, \quad B(z) = B(z_\parallel) = \frac{z_h^4}{z^4(z_h^4 - z^4)} - \frac{1}{(z_h^4 - z^4)(1-a^2)}. \quad (17)$$

The interquark distance  $L$  of  $Q\bar{Q}$  is

$$L = 2 \int_0^{z_c} \sqrt{\frac{A(z_c)B(z)}{A(z)^2 - A(z)A(z_c)}} dz, \quad (18)$$

where  $z_c$  ( $0 < z_c < z_h$ ) is the deepest point of the U-shaped string.

The imaginary potential can be calculated from the thermal fluctuations of the string worldsheet [18], and the expression of the imaginary potential  $ImV$  is

$$ImV = -\frac{\sqrt{\lambda}}{2\sqrt{2}} \sqrt{B(z_c)} \left( \frac{A'(z_c)}{2A''(z_c)} - \frac{A(z_c)}{A'(z_c)} \right), \quad (19)$$

where  $A'(z_c)$  and  $A''(z_c)$  are the first and second derivative of  $A(z_c)$ , respectively.

The thermal width of  $Q\bar{Q}$  is

$$\Gamma/T = -\frac{4}{(a_0 T)^3} \int d\omega \omega^2 e^{\frac{-2\omega}{a_0 T}} \frac{ImV(\omega)}{T}, \quad (20)$$

where  $\omega = LT$  and  $a_0$  is the Bohr radius. There are exact approach and approximate approach to calculate the thermal width [19, 28]. It should be mentioned that the authors of [31] study the effect of gluon condensate on the thermal width by exact approach and approximate approach. The qualitative results from the two approaches are consistent. In this work, we adopt the approximate approach to discuss the effect of angular momentum on the thermal width.

We will examine the effect of angular momentum on the imaginary potential and thermal width in the spinning Myers-Perry black hole from Eqs.(18), (19), and (20). For our calculations, we take  $\lambda = 1$ . According to Ref. [41], the background geometry features a planar

black brane at high temperatures. Therefore, we choose a high temperature  $T = 100/\pi$ . Additionally, the background remains stable when  $a < 0.75L$ . Thus, we take  $a = 0.1, 0.2, 0.3$  in the numerical calculations. It should be mentioned that the spinning background is dual to the rotating QGP system. The behavior of QGP flow can be visualized as a uniform motion, characterized by uniformly rotating circles of a Hopf fibration within the spatial component of four-dimensional spacetime [42].

Then we discuss three restrictions on the imaginary potential. Firstly, the term  $B(z_c)$  in Eq.(19) must be positive. Secondly, the imaginary potential should be negative. This requirement implies that  $(\frac{A'(z_c)}{2A''(z_c)} - \frac{A(z_c)}{A'(z_c)}) > 0$  in Eq.(19), leading to the condition  $\varepsilon > \varepsilon_{min}$  ( $\varepsilon \equiv z_c/z_h$ ). The last restriction is related to the maximum value of  $LT$ , denoted as  $LT_{max}$ . In the left panel of Fig. 1, namely Fig. 1(a), we draw the interquark distance  $LT$  versus  $\varepsilon$  with different values of angular momentum  $a$ . It can be observed that  $LT$  increases monotonically with  $\varepsilon$  and reaches a maximum value,  $LT_{max}$ , at  $\varepsilon = \varepsilon_{max}$ . This feature suggests that the string is a U-shape type. When  $\varepsilon > \varepsilon_{max}$ , the  $LT$  decrease monotonically with  $\varepsilon$ , indicating the string configurations solutions no longer satisfy the Nambu-Goto action [44]. Therefore, we restrict our calculations to the range  $\varepsilon_{min} < \varepsilon < \varepsilon_{max}$  ( $LT_{min} < LT < LT_{max}$ ) in the calculations. We also find that the presence of angular momentum suppresses  $LT_{max}$ , suggesting angular momentum favors the dissociation of quarkonium. Moreover, the dissociation effect is stronger in the transverse cases.

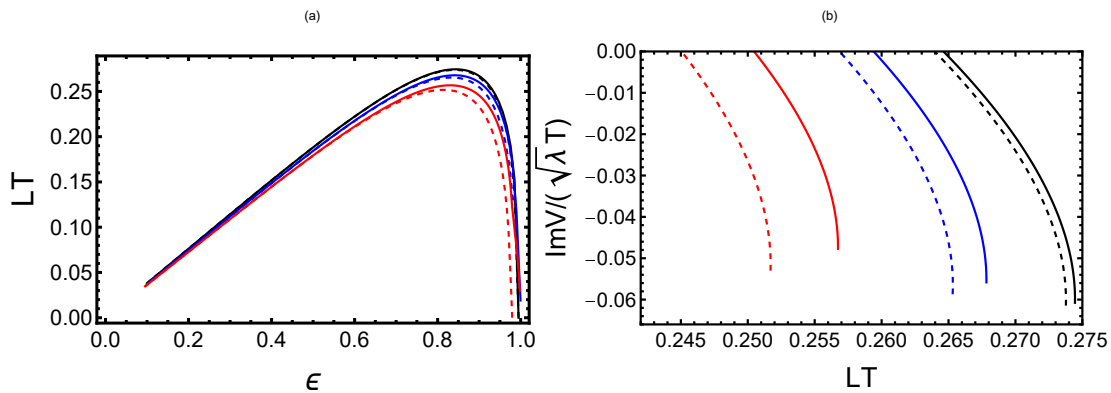


FIG. 1. (a)  $LT$  versus  $\varepsilon$  with different angular momentum  $a$ . (b) Imaginary potential  $ImV/(\sqrt{\lambda}T)$  of quarkonium versus  $LT$  with different angular momentum  $a$ . The black, blue and red line denote  $a = 0.1, 0.2, 0.3$ , respectively. The solid line (dashed line) represents the parallel (transverse) case.

In Fig. 1(b), we depict the imaginary potential  $ImV/(\sqrt{\lambda}T)$  of quarkonium as a function

of  $LT$  with different angular momentum  $a$ . The imaginary potential begins at  $LT_{min}$  and ends at  $LT_{max}$ . It is evident that the imaginary potential appears at smaller  $LT$  as the angular momentum increases. As noted in Ref. [20], the suppression will becomes stronger when the imaginary potential occurs at smaller  $LT$ . Therefore, we can conclude that angular momentum contributes to the melting of quarkonium. Additionally, the impact of angular momentum on the imaginary potential is more significant in the transverse case compared to the parallel case.

The authors of Ref. [27] extend the static black hole to a local rotating by the Lorentz transformation and calculate the imaginary potential in this local rotating background. They find the angular momentum enhances the dissociation. Although the rotating backgrounds considered are different, our results coincide with the results of Ref. [27].

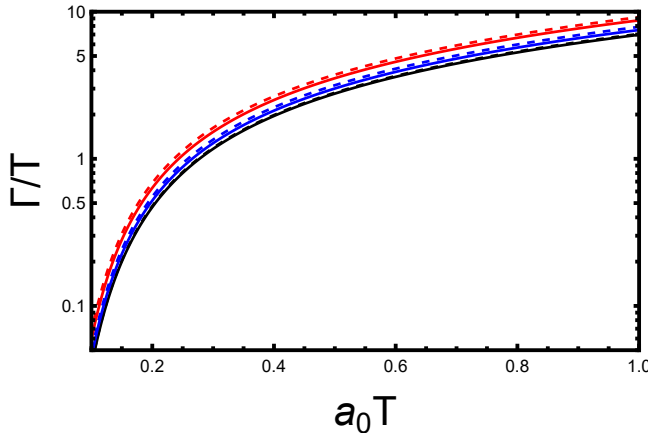


FIG. 2. Thermal width  $\Gamma/T$  versus  $a_0T$  with different angular momentum  $a$ . The black, blue and red line denote  $a = 0.1, 0.2, 0.3$ , respectively. The solid line (dashed line) represents the parallel (transverse) case.

Next, we examine how angular momentum affects thermal width. We plot the thermal width  $\Gamma/T$  against  $a_0T$  for various angular momentum  $a$  in Fig. 2. One can observe that the angular momentum enhances the thermal width, with a more significant effect observed in the transverse case than in the parallel case. A larger thermal width indicates that the state is unstable and may break down into free quarks, whereas a smaller thermal width suggests a more stable bound state. This phenomenon can be explained by the binding energy of heavy quarkonium. The authors of Ref. [45] investigate the thermodynamics of heavy quarkonium in a spinning black hole background and calculate its binding energy. They discover that

the binding energy increases quickly to zero when increasing angular momentum, indicating that heavy quarkonium is more unstable at larger angular momentum. The authors of Ref. [46] examine the spectral function of heavy quarkonium within the same spinning black hole background and find that angular momentum facilitates the dissociation of heavy quarkonium. Our results are consistent with those presented in Refs. [45, 46].

#### IV. CONCLUSION AND DISCUSSION

In this paper, we investigate the imaginary potential and thermal width of heavy quarkonium in the spinning black hole background. The imaginary potential could explain the dissociation and decay of the bound state. Also, it can be used to estimate the thermal width related to thermal decay.

We find that the angular momentum suppresses the maximum value of interquark distance  $LT$ . As angular momentum increases, the imaginary potential appears at smaller  $LT$ , indicating that angular momentum contributes to the melting of quarkonium. Additionally, we observe that angular momentum enhances the thermal width, indicating that the bound state is more unstable at larger angular momentum. Furthermore, we conclude that angular momentum has a stronger effect on the dissociation of quarkonium when the axis of the quark-antiquark pair  $Q\bar{Q}$  is transverse to the direction of angular momentum.

The study of the imaginary potential and thermal width of the heavy quarkonium under rotation is crucial for understanding their behavior in rotating thermal QGP, which contributes to investigate the quarkonium suppression and thermalization in heavy-ion collisions experiments. Finally, investigating configuration entropy within a spinning black hole may be a meaningful work. We plan to delve into this topic in our subsequent studies.

#### ACKNOWLEDGMENTS

Defu Hou's research is supported in part by the National Key Research and Development Program of China under Contract No. 2022YFA1604900. Additionally, he receives partial support from the National Natural Science Foundation of China (NSFC) under Grant No.12435009, and No. 12275104. Zhou-Run Zhu's work is supported by the startup Foundation projects for Doctors at Zhoukou Normal University, with the project number

- [1] T. Matsui and H. Satz, Phys. Lett. B **178**, 416-422 (1986) doi:10.1016/0370-2693(86)91404-8
- [2] M. Laine, O. Philipsen, P. Romatschke and M. Tassler, JHEP **03** (2007), 054 doi:10.1088/1126-6708/2007/03/054 [arXiv:hep-ph/0611300 [hep-ph]].
- [3] A. Beraudo, J. P. Blaizot and C. Ratti, Nucl. Phys. A **806** (2008), 312-338 doi:10.1016/j.nuclphysa.2008.03.001 [arXiv:0712.4394 [nucl-th]].
- [4] Y. Burnier, M. Laine and M. Vepsalainen, Phys. Lett. B **678** (2009), 86-89 doi:10.1016/j.physletb.2009.05.067 [arXiv:0903.3467 [hep-ph]].
- [5] N. Brambilla, M. A. Escobedo, J. Ghiglieri, J. Soto and A. Vairo, JHEP **09** (2010), 038 doi:10.1007/JHEP09(2010)038 [arXiv:1007.4156 [hep-ph]].
- [6] N. Brambilla, J. Ghiglieri, A. Vairo and P. Petreczky, Phys. Rev. D **78** (2008), 014017 doi:10.1103/PhysRevD.78.014017 [arXiv:0804.0993 [hep-ph]].
- [7] M. Margotta, K. McCarty, C. McGahan, M. Strickland and D. Yager-Elorriaga, Phys. Rev. D **83** (2011), 105019 [erratum: Phys. Rev. D **84** (2011), 069902] doi:10.1103/PhysRevD.84.069902 [arXiv:1101.4651 [hep-ph]].
- [8] Z. T. Liang and X. N. Wang, Phys. Rev. Lett. **94** (2005), 102301 [erratum: Phys. Rev. Lett. **96** (2006), 039901] doi:10.1103/PhysRevLett.94.102301 [arXiv:nucl-th/0410079 [nucl-th]].
- [9] F. Becattini, F. Piccinini and J. Rizzo, Phys. Rev. C **77** (2008), 024906 doi:10.1103/PhysRevC.77.024906 [arXiv:0711.1253 [nucl-th]].
- [10] M. Baznat, K. Gudima, A. Sorin and O. Teryaev, Phys. Rev. C **88** (2013) no.6, 061901 doi:10.1103/PhysRevC.88.061901 [arXiv:1301.7003 [nucl-th]].
- [11] L. Adamczyk *et al.* [STAR], Nature **548** (2017), 62-65 doi:10.1038/nature23004 [arXiv:1701.06657 [nucl-ex]].
- [12] Y. Jiang, Z. W. Lin and J. Liao, Phys. Rev. C **94** (2016) no.4, 044910 [erratum: Phys. Rev. C **95** (2017) no.4, 049904] doi:10.1103/PhysRevC.94.044910 [arXiv:1602.06580 [hep-ph]].
- [13] M. I. Baznat, K. K. Gudima, A. S. Sorin and O. V. Teryaev, Phys. Rev. C **93** (2016) no.3, 031902 doi:10.1103/PhysRevC.93.031902 [arXiv:1507.04652 [nucl-th]].
- [14] D. E. Kharzeev, J. Liao, S. A. Voloshin and G. Wang, Prog. Part. Nucl. Phys. **88** (2016), 1-28 doi:10.1016/j.ppnp.2016.01.001 [arXiv:1511.04050 [hep-ph]].

- [15] J. M. Maldacena, Adv. Theor. Math. Phys. **2**, 231-252 (1998) doi:10.1023/A:1026654312961 [arXiv:hep-th/9711200 [hep-th]].
- [16] E. Witten, Adv. Theor. Math. Phys. **2**, 253-291 (1998) doi:10.4310/ATMP.1998.v2.n2.a2 [arXiv:hep-th/9802150 [hep-th]].
- [17] S. S. Gubser, I. R. Klebanov and A. M. Polyakov, Phys. Lett. B **428**, 105-114 (1998) doi:10.1016/S0370-2693(98)00377-3 [arXiv:hep-th/9802109 [hep-th]].
- [18] J. Noronha and A. Dumitru, Phys. Rev. Lett. **103** (2009), 152304 doi:10.1103/PhysRevLett.103.152304 [arXiv:0907.3062 [hep-ph]].
- [19] S. I. Finazzo and J. Noronha, JHEP **11** (2013), 042 doi:10.1007/JHEP11(2013)042 [arXiv:1306.2613 [hep-ph]].
- [20] S. I. Finazzo and J. Noronha, JHEP **01** (2015), 051 doi:10.1007/JHEP01(2015)051 [arXiv:1406.2683 [hep-th]].
- [21] M. Ali-Akbari, D. Giataganas and Z. Rezaei, Phys. Rev. D **90** (2014) no.8, 086001 doi:10.1103/PhysRevD.90.086001 [arXiv:1406.1994 [hep-th]].
- [22] K. B. Fadafan and S. K. Tabatabaei, Eur. Phys. J. C **74** (2014), 2842 doi:10.1140/epjc/s10052-014-2842-2 [arXiv:1308.3971 [hep-th]].
- [23] K. Bitaghsir Fadafan and S. K. Tabatabaei, J. Phys. G **43** (2016) no.9, 095001 doi:10.1088/0954-3899/43/9/095001 [arXiv:1501.00439 [hep-th]].
- [24] J. Sadeghi and S. Tahery, JHEP **06** (2015), 204 doi:10.1007/JHEP06(2015)204 [arXiv:1412.8332 [hep-th]].
- [25] N. R. F. Braga and L. F. Ferreira, Phys. Rev. D **94** (2016) no.9, 094019 doi:10.1103/PhysRevD.94.094019 [arXiv:1606.09535 [hep-th]].
- [26] Z. q. Zhang and X. Zhu, Phys. Lett. B **793** (2019), 200-205 doi:10.1016/j.physletb.2019.04.057
- [27] Z. q. Zhang, X. Zhu and D. f. Hou, Nucl. Phys. B **989** (2023), 116149 doi:10.1016/j.nuclphysb.2023.116149
- [28] K. Bitaghsir Fadafan, D. Giataganas and H. Soltanpanahi, JHEP **11** (2013), 107 doi:10.1007/JHEP11(2013)107 [arXiv:1306.2929 [hep-th]].
- [29] Z. q. Zhang, D. f. Hou and G. Chen, Phys. Lett. B **768** (2017), 180-186 doi:10.1016/j.physletb.2017.02.055 [arXiv:1612.08826 [hep-th]].
- [30] Z. q. Zhang and D. f. Hou, Phys. Lett. B **778** (2018), 227-232 doi:10.1016/j.physletb.2018.01.028 [arXiv:1802.01919 [hep-th]].

- [31] Y. Q. Zhao, Z. R. Zhu and X. Chen, Eur. Phys. J. A **56** (2020) no.2, 57 doi:10.1140/epja/s10050-020-00072-5 [arXiv:1909.04994 [hep-ph]].
- [32] M. Kioumarsipour and J. Sadeghi, Eur. Phys. J. C **81** (2021) no.8, 735 doi:10.1140/epjc/s10052-021-09537-3 [arXiv:2210.13919 [hep-th]].
- [33] M. Kioumarsipour and B. Khanpour, Phys. Lett. B **855** (2024), 138791 doi:10.1016/j.physletb.2024.138791 [arXiv:2406.13792 [hep-th]].
- [34] J. L. Albacete, Y. V. Kovchegov and A. Taliotis, Phys. Rev. D **78** (2008), 115007 doi:10.1103/PhysRevD.78.115007 [arXiv:0807.4747 [hep-th]].
- [35] C. Erices and C. Martinez, Phys. Rev. D **97** (2018) no.2, 024034 doi:10.1103/PhysRevD.97.024034 [arXiv:1707.03483 [hep-th]].
- [36] M. Bravo Gaete, L. Guajardo and M. Hassaine, JHEP **04** (2017), 092 doi:10.1007/JHEP04(2017)092 [arXiv:1702.02416 [hep-th]].
- [37] A. M. Awad, Class. Quant. Grav. **20** (2003), 2827-2834 doi:10.1088/0264-9381/20/13/327 [arXiv:hep-th/0209238 [hep-th]].
- [38] S. W. Hawking, C. J. Hunter and M. Taylor, Phys. Rev. D **59**, 064005 (1999) doi:10.1103/PhysRevD.59.064005 [arXiv:hep-th/9811056 [hep-th]].
- [39] G. W. Gibbons, M. J. Perry and C. N. Pope, Class. Quant. Grav. **22**, 1503-1526 (2005) doi:10.1088/0264-9381/22/9/002 [arXiv:hep-th/0408217 [hep-th]].
- [40] G. W. Gibbons, H. Lu, D. N. Page and C. N. Pope, Phys. Rev. Lett. **93**, 171102 (2004) doi:10.1103/PhysRevLett.93.171102 [arXiv:hep-th/0409155 [hep-th]].
- [41] M. Garbiso and M. Kaminski, JHEP **12**, 112 (2020) doi:10.1007/JHEP12(2020)112 [arXiv:2007.04345 [hep-th]].
- [42] M. A. G. Amano, C. Cartwright, M. Kaminski and J. Wu, Prog. Part. Nucl. Phys. **139** (2024), 104135 doi:10.1016/j.ppnp.2024.104135 [arXiv:2308.11686 [hep-th]].
- [43] K. Murata, Prog. Theor. Phys. **121**, 1099-1124 (2009) doi:10.1143/PTP.121.1099 [arXiv:0812.0718 [hep-th]].
- [44] D. Bak, A. Karch and L. G. Yaffe, JHEP **08** (2007), 049 doi:10.1088/1126-6708/2007/08/049 [arXiv:0705.0994 [hep-th]].
- [45] Z. R. Zhu, S. Wang, X. Chen, J. X. Chen and D. Hou, Phys. Rev. D **110** (2024) no.12, 126008 doi:10.1103/PhysRevD.110.126008 [arXiv:2407.03633 [hep-ph]].

- [46] Z. R. Zhu, M. Sun, R. Zhou, Z. Ma and J. Han, Eur. Phys. J. C **84** (2024) no.12, 1252  
doi:10.1140/epjc/s10052-024-13628-2 [arXiv:2406.19661 [hep-ph]].